FLOW OVER THICK AIRFOILS IN GROUND EFFECT – AN INVESTIGATION ON THE INFLUENCE OF CAMBER

Ahmed M. Rafiuddin
Department of Engineering, The University of the South Pacific, Suva, Fiji

Abstract

Results from an experimental investigation of aerodynamic ground effect on three airfoils, NACA 0015, 4415 and 6415, carried out in a low speed wind tunnel are presented. The pressure distribution on the airfoil surface was obtained from pressure tappings. Mean velocity measurements were performed over the surface of the airfoil and velocity contours were plotted. Measurements of mean velocity and turbulence intensities were performed in the wake region at two locations. Experiments were carried out by varying the angle of attack from 0^0 to 10^0 and ground clearance from the minimum possible value to one chord length. It was found that high values of pressure coefficient are obtained on the lower surface when the airfoil is close to the ground. This region of high pressure extended almost over the entire chord length for higher angles of attack. The flow was found to accelerate over the airfoils with the highest acceleration observed for NACA 4415 and lowest for NACA 6415. For NACA 4415 model, a very high mean velocity is observed near the suction peak location. For this airfoil, the flow was found to separate from the surface for angles of attack 10^0 and above, resulting in considerably lower velocities over the surface and a thick and highly turbulent wake region.

1 Introduction

The flow around an airfoil or a wing is considerably modified under the influence of ground effect. The dividing streamline and the stagnation point move down, hence more air flows above the wing; thus there is a decrease in velocity below the wing and an increase in pressure, resulting in an air cushion effect. The streamline patterns over the leading and trailing edges of a wing in ground effect can be seen in ref. [1]. For very small clearances, the air tends to stagnate under the wing, which will give the highest possible pressure, so called ram pressure, resulting in a considerable increase in lift. Simultaneously, the induced drag for wing is lowered as the induced downwash velocity diminishes close to the ground.

The streamline modification has interesting consequences - the effective angle of attack increases, which causes an increase in lift force; on the other hand, the absence of downwash reduces the drag, which otherwise increases with angle of attack. The effects of proximity to ground for an airfoil on the lift and drag characteristics were studied as early as in 1920s [2,3]. The increased lift and reduced drag can be used to increase flight range at a reduced specific fuel consumption compared to the conventional aircraft. Besides, the WIG vehicle has other advantages over a conventional mode of air transport such as less energy consumption during take-off, no need of pressurized cabin, smaller infrastructure and safer runway because it is near the ground. There have been some successful attempts to develop WIG vehicles that fly overwater. A review of the various types of vehicles experimented at various times is made by Ollila [4]. Ando [5] made a critical review of the design philosophies of overwater transport WIG vehicles. Work on development of overwater WIG vehicles is currently going on in many countries; the potential fuel savings and speed advantages over other modes of water transport providing the impetus.

The development of the WIG vehicles for possible applications in both overwater and overland transport necessitates a thorough investigation of the flow characteristics over the wings and other lifting surfaces. There have been some experimental as well as theoretical studies on influence of different wing configurations on the aerodynamic characteristics [6-13]. Studies performed by Ranzenbach and Barlow [6-8] demonstrated the ground effect for a single element airfoil configuration. They performed experiments and did numerical studies on single element symmetrical and cambered airfoils. They found that the lift force reaches a maximum at a ground clearance of approximately 0.08c; beyond this the airfoil and ground boundary layers were found to merge, which was given as the explanation for reduced lift force very close to the ground. Although they documented the effect of ground proximity on the lift and drag forces, no other data was presented.

Ahmed and Kohama [9] presented results of an experimental investigation on a tandem wing configuration. They studied the influence of wing spacing in addition to the effects of angles of attack for the two wings and their ground clearances. Zhang et al [10] reported the influence of tip vortex characteristics on the aerodynamic performance of a cambered airfoil. Zerihan and Zhang [11] reported pressure coefficient and lift and drag coefficient values on an airfoil provided with end plates. They found that at moderate clearances, separation of the boundary layer occurred near the trailing edge of the suction surface. The region of separated flow was found to increase in size as the airfoil was brought very close to the ground. In another paper, Zhang and Zerihan [12] investigated the wake behind a single element airfoil using laser anemometry. They found a thicker wake with reducing ground proximity, as a result of boundary layer separation. Recently, Ahmed and Goonaratne [13] reported increasing values of coefficients of lift and drag with angle of attack. They also reported increasing lift coefficient values and decreasing drag coefficient values as the ground was approached for an angle of attack of 2^0 and

different flap angles. So, it can be seen that some studies have involved surface pressure measurements and a few studies have explored wake and tip vortices. Scarcity of published work on surface pressures, mean velocity distribution over the surface, and wake survey to clearly understand the flow structure for different airfoil configurations prompted the present work.

The present paper deals with a study of the aerodynamic characteristics - pressure distribution on the surface of the airfoil, mean velocity distribution over the surface of the airfoil and mean velocity and turbulence intensity distributions in the wake region for three NACA airfoils for different angles of attack and for different ground clearances.

The flow structure over an airfoil does not show significant variation with Reynolds number at low angles of attack, as the separation points are fixed close to the trailing edge. The lift slope is not found to be influenced by Reynolds number [14]. The drag coefficient at higher angles of attack is sensitive to Reynolds number, as both skin friction and flow separation are viscous effects [14]. Hence, the present work provides valuable data and information on the influence of camber on the flow structure over airfoils in ground effect. The main objectives of the present work are: (a) to study the pressure distribution over the wing surface at different ground clearances and angles of attack and to measure the lift and drag forces and (b) to study the mean flow over the surface of the wing and to follow the flow in the wake region for mean and fluctuating velocities.

2 Experimental Method

2.1 Wind Tunnel

The experiments were carried out at a velocity of 35 *m/s* in an open circuit, suction type, low speed wind tunnel. The air flow in the tunnel was generated by a single stage axial flow fan having a rated discharge of 216 m³/min at the total pressure of 101.172 kPa and driven by a thyristor controlled 3.75 kW DC motor having a

maximum speed of 2800 rpm. A velocity range of 5 *m/s* to 40 *m/s* can be realized in the square test section having a cross section of 300 *mm* x 300 *mm* and a length of 1 m. The test section is provided with perspex windows on both sides. A traversing mechanism is provided on top of the test section for moving the pitot tube and the hot-wire anemometer probe along its length, as shown in Fig. 1. A settling chamber, provided with honeycomb gauges and four M.S. screens of 18, 30, 50 and 100 mesh, was used for correcting the flow. A bell-mouthed entry ensured smooth entry of the air to the settling chamber. The airflow was discharged into the test section through the square outlet of the contraction, having a width of 900 *mm* at the inlet. The area ratio of the contraction nozzle is 9:1. The freestream turbulence intensity in the test section at the above velocity was found to be 0.8%.
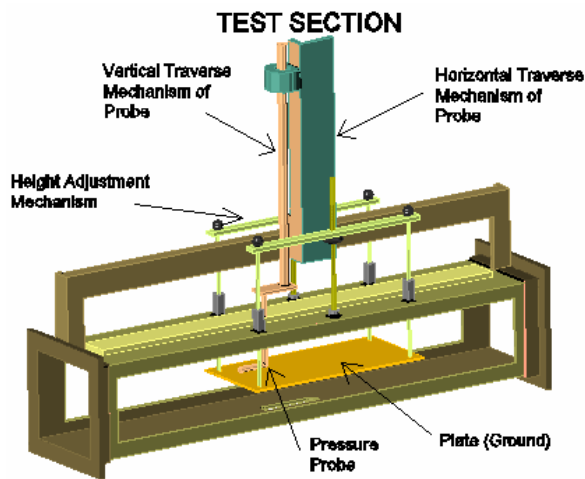
Fig. 1   A schematic diagram of the test section

2.2 Mechanism for Varying the Ground Clearance

To simulate the ground, a flat plate was used inside the test section and this plate was moved up and down to maintain the desired ground clearance. The plate can be moved vertically in the test section with the help of a nut and bolt mechanism provided at the top of the test section, as shown in Fig. 1. The length of the plate was 400 *mm* and it was as wide as the test section to make sure that no flow leakage takes place in the spanwise direction.

The desired ground clearance was obtained by adjusting the lengths of the four rods supporting the plate from the four corners with the help of the screws provided. Although the ground (plate) was fixed in the present investigation, every care was taken to simulate the true ground effect. The boundary layer thickness on the plate at the location of the leading edge of the airfoil was about 1 *mm*. It was found from measurements that both the plate and wing boundary layers are turbulent. Upstream of the airfoil, the ground plate length was slightly more than the length of the chord length of the airfoil. Initial studies involving smoke injection were performed to make sure that at the angles of attack of interest, streamlines did not divert under the plate due to interference.

2.3 Test Model and Experimental Set-up

The airfoils chosen for the present work were NACA 0015, NACA 4415 and NACA 6415, a maximum thickness of 15% for all airfoils and cambers of 0%, 4% and 6% for the three airfoils respectively. These profiles were chosen as it is near this thickness that maximum lift coefficient is obtained [14]. All airfoils have a chord length of 100 *mm* and span of 300 *mm*, which is equal to the width of the test section, thus eliminating wingtip vortices and hence the third component. Pressure taps were provided on both sides of the airfoil, as shown in Fig. 2. However, pressure measurements were performed for NACA 0015 and NACA 6415 models only. The airfoil was mounted in the test section with the help of two pegs provided at the ends which exactly fitted into the holes provided on the two side windows of the test section.
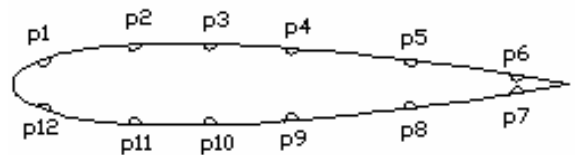

Fig. 2 Locations o f pressure tappings

The airfoils could be held at any desired angle of attack using a round protractor provided with a screw mechanism. A slot was

provided in the top wall of the test section for passing the impact tube and the hot wire probe. A two component hot-wire anemometry system, consisting of two constant temperature anemometer (CTA) units, two signal conditioners, a mean value unit and an RMS unit was used for the current investigations. A tungsten wire of diameter 5 microns and a length of 2 *mm* served as the hot-wire. As the WIG craft fly at low angles of attack, measurements were limited to an angle of attack of 10^0. A maximum blockage ratio of about 6% was found for this angle of attack. A correction factor for the solid and wake blockage, ε, equal to a quarter of the ratio of the total frontal area and the test section area, was employed following ref. [13,15]. The measured freestream velocity was corrected for the total blockage effect [15].

2.4 Experimental Procedure

An impact tube was used for measuring the total pressure. The pressure was read at a U-tube water manometer as well as on a digital pressure indicator. The static pressure was measured on the wall of the wind tunnel and the dynamic pressure head was calculated with the help of this static pressure. For measuring the pressure at different points on the airfoil, a multi-tube, inclined manometer was used. The bottom of all the tubes are interconnected, which in turn, are connected to the balancing reservoir.

The hot-wire anemometer was calibrated against the impact tube. All measurements in the present investigation were performed at a freestream mean velocity of 35 *m/s*. The Reynolds number, based on the corrected velocity and the chord length of the airfoil, was 0.24×10^6.

The model was held in the test section with the help of slots provided on both sides of the test section, and the required angle of attack was set. The required velocity was set with the help of the thyristor speed control system. The readings from the multibank manometer were noted. The manometer board was set at an angle of 20^0 with the vertical for all pressure measurements. Experiments were performed by varying the angle of attack, α, from 0^0 to 10^0. The ground clearance of the trailing edge of the airfoil (h) was varied from the minimum possible value to 90 *mm*, giving h/c values of upto 0.9. For lower angles of attack, measurements at small values of *h* could not be performed as the thicker part of the airfoil was touching the ground plate. Thus, at the angle of attack of 0^0, the minimum value of *h* obtained was 8.5 *mm*. In the wake region, hot-wire probe was traversed from 3 *mm* above the plate to nearly 100 *mm* at two axial locations of 50 *mm* and 100 *mm* from the trailing edge of the airfoil model.

3 Results and Discussion

The results are presented and discussed in this section. For calculation of Coefficient of pressure (C_P), the measured static pressure at a location was non-dimensionalized with respect to the freestream static pressure and the corrected freestream mean velocity (U_∞). All mean and fluctuating velocities are non-dimensionalized with respect to the corrected freestream mean velocity (U_∞).

3.1 Surface Pressure Distribution

Figures 3 through 13 show the variation of Cp on the surface of the airfoils for different angles of attack. The symbol ◆ is used for the lower surface and ▲ for the upper surface. Figure 3 shows the variation in Cp on NACA 0015 airfoil surface for the angle of attack of 0° and a ground clearance (h/c) of 0.085. It is interesting that, due to ramming action, the pressure is quite high on the lower surface, considering the fact that it is a symmetrical airfoil.
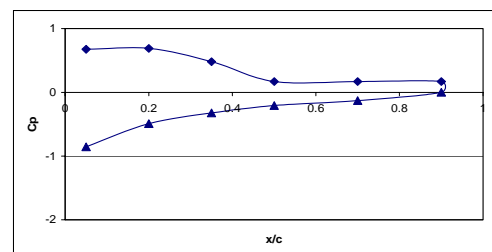

Fig. 3 Pressure distribution on the surface of NACA 0015 airfoil for α = 0^0 and h/c = 0.085

A very interesting observation in these measurements is a suction effect on the lower surface at ground clearances of h/c = 0.1 to h/c = 0.25, although the pressure is positive at the first measurement point. Figure 4 shows the pressure distribution on the surface of the airfoil at a ground clearance of 0.15.
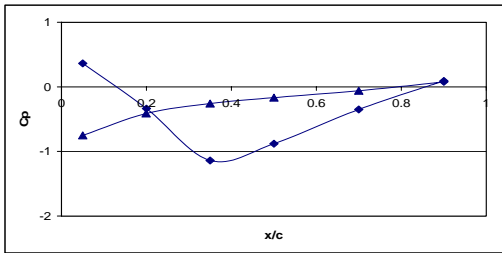

Fig. 4 Pressure distribution on the surface of NACA 0015 airfoil for $\alpha = 0^0$ and h/c = 0.15

This is because the area below the wing forms a convergent-divergent passage, hence, the pressure reduces near the location of minimum area and again increases. This phenomenon is observed till an angle of attack of 5^0, beyond which there is only a diverging path below the wing. As the ground clearance is increased, the value of Cp at the first location starts decreasing and at higher values of h/c, the value of Cp becomes negative at this location and does not show much variation with h/c. Figure 5 shows the pressure distribution for the ground clearance of h/c = 0.85. For this ground clearance, the streamlines converge on both the sides and from the symmetry of the airfoil, similar pressure distribution is obtained on both sides of the airfoil.
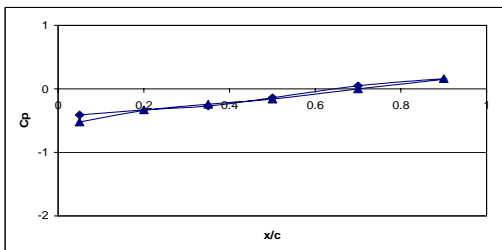
Fig. 5 Pressure distribution on the surface of NACA 0015 airfoil for $\alpha = 0^0$ and h/c = 0.85

The pressure distribution on the surface of the NACA 0015 airfoil for an angle of attack of 2.5^0 and a ground clearance (h/c) of 0.05 is shown in Fig. 6. The pressure coefficient is

positive at all the points on the lower surface, while on the upper surface, stronger suction effect compared to the 0^0 case was observed. A suction effect on the lower surface due to the formation of a convergent-divergent path below the airfoil can clearly be seen from Fig. 7 for the ground clearance of h/c = 0.15. This effect was stronger for the angle of attack of 0^0.
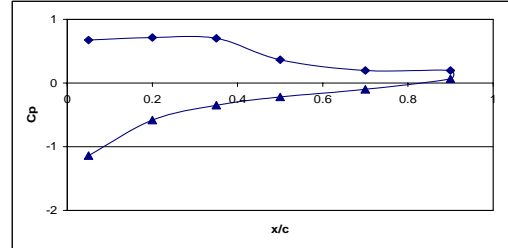

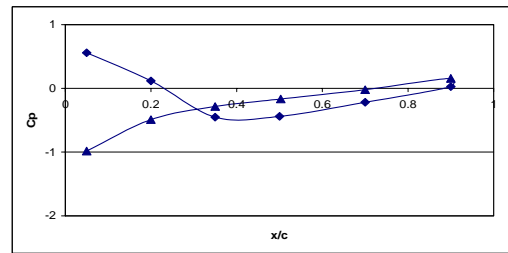Fig. 6 Pressure distribution on the surface of NACA 0015 airfoil for $\alpha = 2.5^0$ and h/c = 0.05

Fig. 7 Pressure distribution on the surface of NACA 0015 airfoil for $\alpha = 2.5^0$ and h/c = 0.15

Zerihan and Zhang [11] reported suction effect on the lower surface; however, they did not provide explanation for this. A small effect of convergent-divergent passage was observed for the angle of attack of 5^0 also; however, the results for this angle of attack are not being presented in this paper.

For the angles of attack of 7.5^0 and above, there is no divergent path under the wing and due to the ramming action, a very high value of Cp is recorded on the lower surface throughout the chord length of the airfoil. The Cp value at the first measurement location on the suction side is high negative (corresponding to the suction peak) and increases to a value of about 0.1 at the last measurement point close to the trailing edge, due to which there is a reduction in velocity as we move downstream. Figure 8 shows the pressure distribution for this angle of attack at a ground clearance of h/c = 0.02.
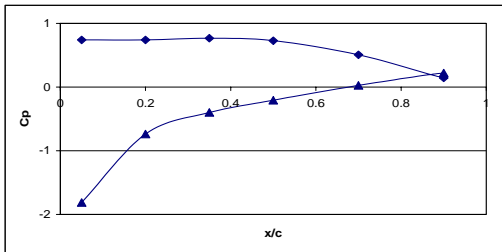
Fig. 8 Pressure distribution on the surface of NACA 0015 airfoil for $\alpha = 7.5^0$ and h/c = 0.02

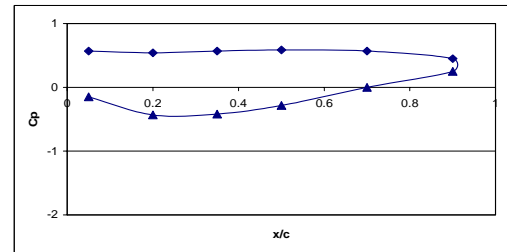When the angle of attack is increased to 10^0, the pressure on the lower surface further increases, as can be seen from Fig. 9. The value of Cp is close to one almost till the trailing edge.
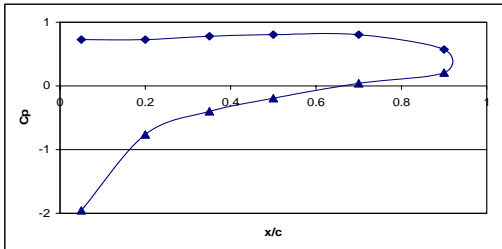

Fig. 9 Pressure distribution on the surface of NACA 0015 airfoil for $\alpha = 10^0$ and h/c = 0.0

For the NACA 6415 airfoil, there is a suction effect on the lower surface for smaller angles of attack (upto 5^0) at the first measurement location. The pressure distribution for the angle of attack of 5^0 for a ground clearance of h/c = 0.04 is shown in Fig. 10. Except for the first measurement location, the pressure coefficient is positive at all points on the lower surface of the airfoil.
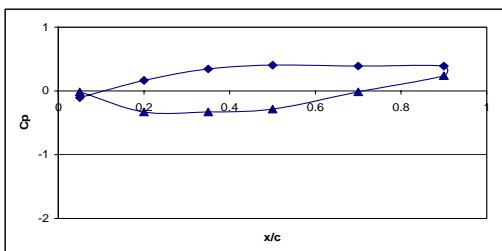

Fig. 10 Pressure distribution on the surface of NACA 6415 airfoil for $\alpha = 5^0$ and h/c = 0.04

When the angle of attack is increased beyond 5^0, the pressure coefficient at the first location on the lower surface becomes positive and on the upper surface negative, as can be seen from Fig. 11 for an angle of attack of 7.5^0 and a ground clearance of h/c = 0.002.

Fig. 11 Pressure distribution on the surface of NACA 6415 airfoil for $\alpha = 7.5^0$ and h/c = 0.002

The high pressure on the lower surface reduces as the ground clearance is increased. The suction pressure on the upper surface at the first measurement location remains nearly the same for all ground clearances. Due to this, a consistently low acceleration of flow is observed over the upper surface. The value of pressure coefficient at the last measurement point (x/c = 0.9) also remains nearly the same for all values of ground clearance. Figure 12 shows the reduced pressure on the lower surface for the higher ground clearance (h/c) of 0.75.
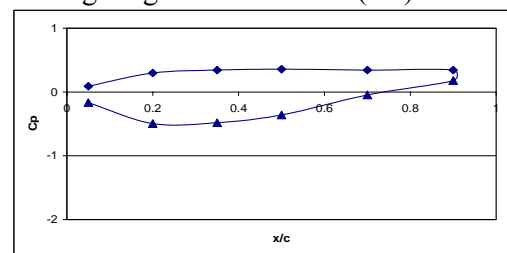

Fig. 12 Pressure distribution on the surface of NACA 6415 airfoil for $\alpha = 7.5^0$ and h/c = 0.75

For the angle of attack of 10^0 and a ground clearance of zero, the pressure is very high throughout the lower surface of the airfoil due to the ramming effect, as can be seen from Fig. 13. A comparison with Fig. 9 indicates that the suction effect is much less compared to the symmetrical airfoil. As the ground clearance is increased, aerodynamic ground effect reduces.
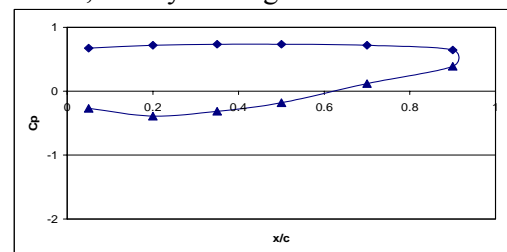

Fig. 13 Pressure distribution on the surface of NACA 6415 airfoil for $\alpha = 10^0$ and h/c = 0.0

3.2 Velocity distribution over the airfoil

Measurements of mean velocity were performed above the airfoil surface from a height (y) of 3 *mm* to about 80 *mm* to study the accelerated flow there. The distributions of mean velocity for the three airfoils for an angle of attack of 7.5^0 and a ground clearance (h/c) of 0.1 are shown in Figs. 14 to 16.

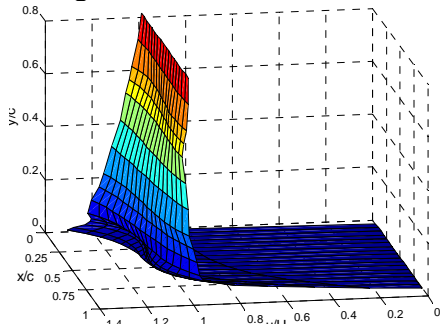Fig. 14 Mean velocity distribution over NACA 0015 airfoil for $\alpha = 7.5^0$ and h/c = 0.1

As can be seen, the flow accelerates over all the airfoils with the maximum increase for the NACA 4415 model. The velocity increased by about 30% for NACA 0015 and by more than 50% for NACA 4415 airfoil. The velocity may be further high close to the surface, but measurements were not made due to possible breakage of the hot wire. The increase is least for NACA 6415 airfoil, as can be seen from Fig. 16. As was discussed in previous section (Figs. 11 and 12), the suction on the upper surface is small for the NACA 6415 model, which is the cause for this least increase in velocity. A gradual reduction in velocity towards the trailing edge, along the chord length of the airfoil, can be seen from all velocity contours.
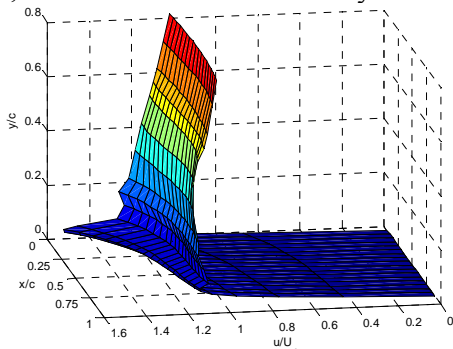

Fig. 15 Mean velocity distribution over NACA 4415 airfoil for $\alpha = 7.5^0$ and h/c = 0.1
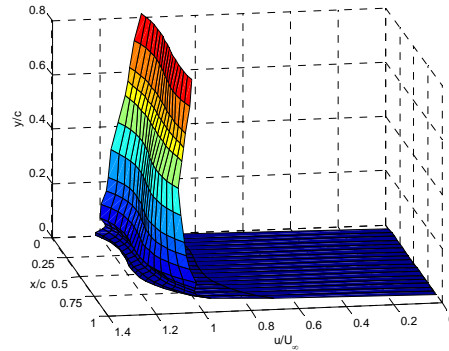

Fig. 16 Mean velocity distribution over NACA 6415 airfoil for $\alpha = 7.5^0$ and h/c = 0.1

Interesting observations were made for the angle of attack of 10^0. The increased suction effect on the upper surface for NACA 0015 airfoil results in considerable acceleration of flow over the surface, as shown in Fig. 17. For NACA 4415 airfoil, the flow separates from the upper surface, as shown from Fig. 18.
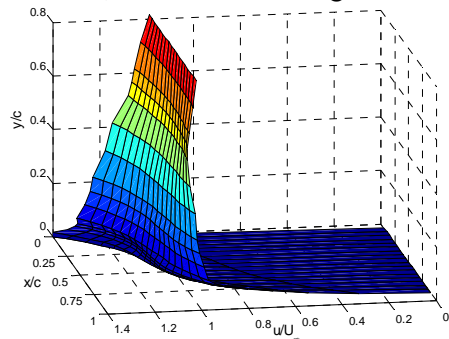

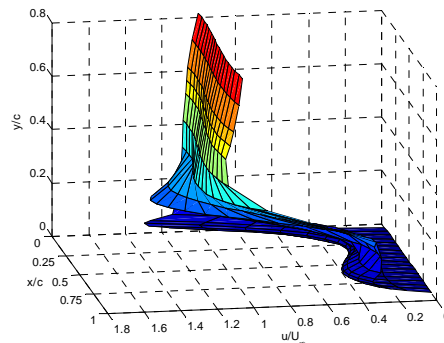Fig. 17 Mean velocity distribution over NACA 0015 airfoil for $\alpha = 10^0$ and h/c = 0.1

Fig. 18 Mean velocity distribution over NACA 4415 airfoil for $\alpha = 10^0$ and h/c = 0.1

The acceleration is minimum for NACA 6415 airfoil, as shown in Fig. 19. It can be inferred that the presence of the airfoil affects the velocity field almost up to half the chord length distance in the vertical direction.
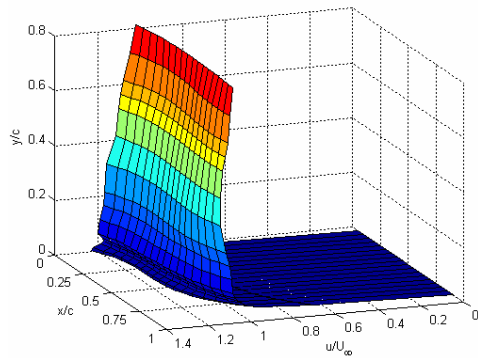
Fig. 19 Mean velocity distribution over NACA 6415 airfoil for $\alpha = 10^0$ and h/c = 0.1

3.3 Wake Survey

Distributions of mean velocity and turbulence intensity in the wake region were plotted by making measurements at ground clearances ranging from the minimum possible value of h/c for that particular angle of attack to h/c = 0.5 from 3 *mm* above the ground plate to about 100 *mm*. The distributions of mean velocity and turbulence intensity for NACA 0015 and 4415 airfoils for an angle of attack of 7.5^0 and small ground clearances are shown in Figs. 20 and 21.
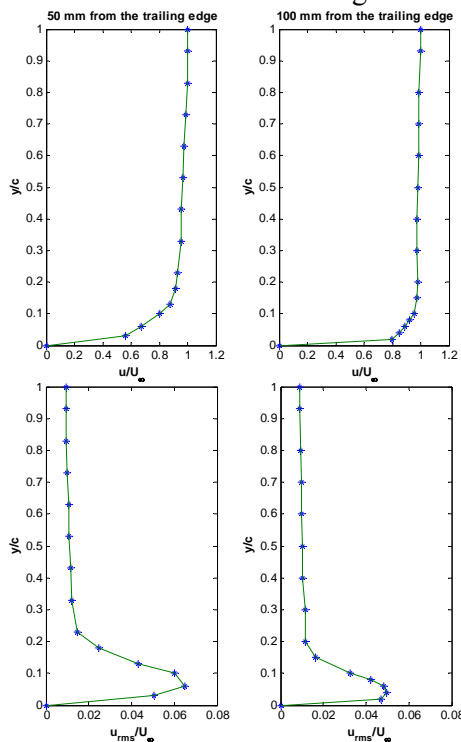

Fig. 20 Distributions of mean velocity and streamwise turbulence intensity in the wake region of NACA 0015 airfoil for $\alpha = 7.5^0$ and h/c = 0.02

The turbulence levels for NACA 0015 airfoil are seen to be very high. The results for this angle of attack and ground clearance for NACA 6415 airfoil are not being shown as the wake region is very thin for this airfoil and the turbulence levels are low.
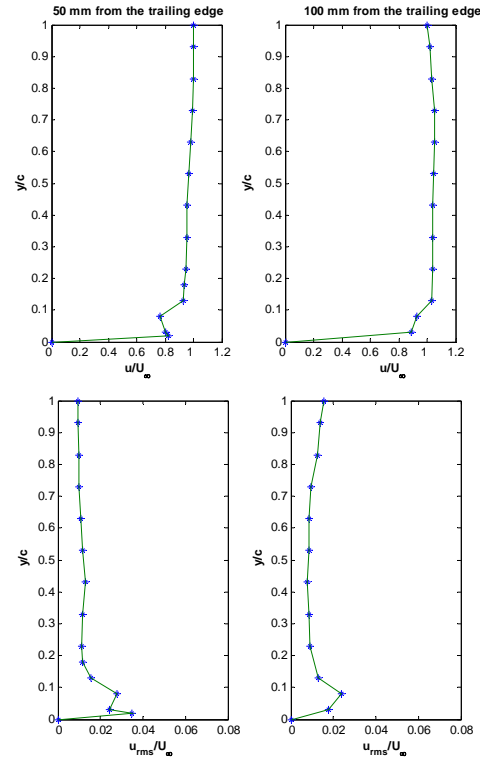

Fig. 21 Distributions of mean velocity and streamwise turbulence intensity in the wake region of NACA 4415 airfoil for $\alpha = 7.5^0$ and h/c = 0.05

The boundary layer which develops over the surface of the airfoil leaves the surface near the trailing edge. This flow reattaches to the ground plate. Due to this, there is a reduction in velocity in that region, and hence a higher momentum loss.

For very low ground clearances, the boundary layers of the plate and the airfoil are found to merge. For values of ground clearance of about 0.1, the boundary layer is penetrated by the accelerating stream, and hence the defect in velocity is not very large. The spreading of the high turbulence region can also be seen from the figure. For a ground clearance of h/c = 0.05 for the angle of attack of 10^0, a slight distinction between the two shear regions can be made from the velocity and turbulence profiles at the

first location. As the passage under the wing acts like a nozzle for this angle, the velocity defect is not large, which results in a lesser drag for this case. The two shear regions merge as we move downstream to a location of l/c = 1.0, as can be seen from Fig. 22.
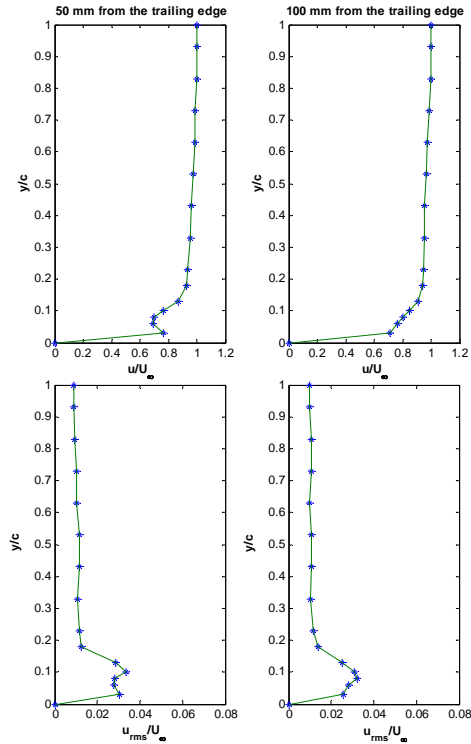

Fig. 22 Distributions of mean velocity and streamwise turbulence intensity in the wake region of NACA 0015 airfoil for $\alpha = 10^0$ and h/c = 0.05

Interference of the wake region with the ground plate is seen to be prominent from this figure. At higher angle of attack, the interaction between the flow leaving the trailing edge and the ground plate causes an increase in the turbulence level.

For NACA 4415 airfoil, as discussed earlier, the flow separates from the upper surface (shown in Fig. 18) resulting in a thick and turbulent wake. The profiles are depicted in Fig. 23. A high turbulence level of about 12% was recorded for this case. As can be seen from the figures, the shear region is as thick as 70% of the airfoil chord length. For the NACA 6415 airfoil, the flow remains attached to the upper surface till very close to the trailing edge, as was discussed earlier. Hence, a thin wake for this case can be seen from Fig. 24.
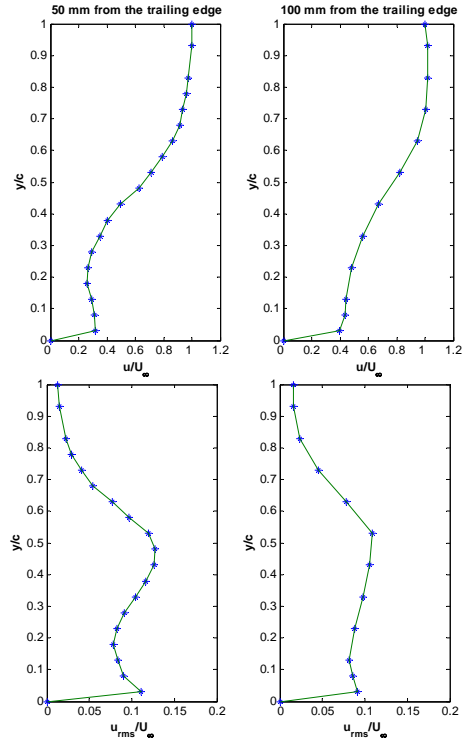

Fig. 23 Distributions of mean velocity and streamwise turbulence intensity in the wake region of NACA 4415 airfoil for $\alpha = 10^0$ and h/c = 0.05
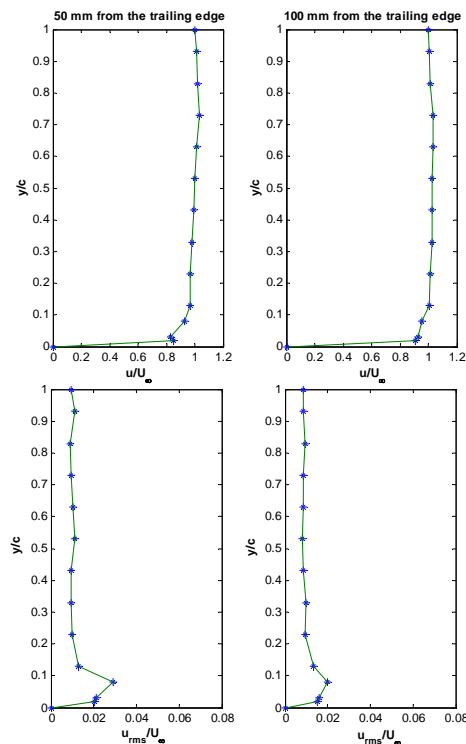

Fig. 24 Distributions of mean velocity and streamwise turbulence intensity in the wake region of NACA 6415 airfoil for $\alpha = 10^0$ and h/c = 0.05

4 Conclusions

The important conclusions drawn from the present work are:

i) The angle of attack and the ground clearance of the airfoil have a strong influence on the aerodynamic characteristics of the configuration. A high pressure region is formed under the wing at lower ground clearances, where the pressure becomes nearly equal to the stagnation pressure at higher angles of attack.

ii) For low ground clearances, as the passage below the airfoil is small, the flow gets diverted over the airfoil. Thus, the flow accelerates over the airfoil, and a considerably higher mean velocity is observed near the suction peak location.

iii) For thick symmetrical airfoils, there is a convergent-divergent path below the wing at lower angles of attack for low ground clearances, which gives rise to suction below the airfoil - which is not a desirable phenomenon. It is advisable to have a flatter bottom surface to reduce this suction effect.

iv) For thick airfoils, the boundary layer leaving the surface reattaches the ground plate slightly downstream of the trailing edge for lower ground clearances. This gives rise to a larger velocity defect and higher levels of turbulence. As the angle of attack is increased, the velocity defect and turbulence levels increase.

v) At slightly higher ground clearances (h/c of about 0.1), there is a local blowing effect under the airfoil, which prevents the boundary layer development on the ground plate.

References

[1] Rozhdestvensky, K *Aerodynamics of a lifting system in extreme ground effect.* 1st edition, Springer-Verlag, p. 30, 2000.

[2] Raymond, A. Ground influence on airfoils. *NACA Technical Note 67*, 1921.

[3] Reid, E. A full scale investigation of ground effect. *NACA Technical Report 265*, 1927.

[4] Ollila, R. Historical review of WIG vehicles. *Journal of Hydronautics*, Vol. 14 No. 3, pp. 65-76, 1980.

[5] Ando, S. Critical review of design philosophies for recent transport WIG effect vehicles. *Trans. Japan Society for Aeronautical and Space Sciences*, Vol. 33, No. 99, pp. 28-40, 1990.

[6] Ranzenbach, R. and Barlow, J. Two-dimensional airfoil in ground effect, an experimental and computational study. *SAE Paper No. 94-2509*, 1994.

[7] Ranzenbach, R. and Barlow, J., Cambered aerofoil in ground effect: wind tunnel and road conditions. *AIAA Paper 95-1909*, 1995.

[8] Ranzenbach, R. and Barlow, J., Cambered aerofoil in ground effect, an experimental and computational study. *SAE Paper No. 96-0909*, 1996.

[9] Ahmed, M. and Kohama, Y., Experimental investigation on the aerodynamic characteristics of a tandem wing configuration in close ground proximity. *JSME International Journal*, Vol. 42, No. 4, pp. 612-618, 1999.

[10] Zhang, X., Zerihan, J., Ruhrmann, A. and Deviese, M. Tip vortices generated by a wing in ground effect. *Proceedings of the 11th International Symposium on Applications of Laser Techniques to Fluid Mechanics*, Portugal, 2002.

[11] Zerihan, J. and Zhang, X. Aerodynamics of a single element wing in ground effect. *Journal of Aircraft*, Vol. 37, No. 6, pp. 1058-1064, 2000.

[12] Zhang, X. and Zerihan, J. Turbulent wake behind a single element wing in ground effect. *Proceedings of the 11th international symposium on applications of laser techniques to fluid mechanics*, Portugal, 2002.

[13] Ahmed, N. and Goonaratne, J. Lift augmentation of a low-aspect-ratio thick wing in ground effect. *Journal of Aircraft*, Vol. 39, No. 2, pp. 381-384, 2002.

[14] Anderson, J. Jr. *Fundamentals of aerodynamics.* 3rd edition, McGraw-Hill, 2001.

[15] Barlow, J., Rae, W. and Pope, A. *Low-speed wind tunnel testing.* 3rd edition, John Wiley, 1999.